Contents lists available at ScienceDirect

Microporous and Mesoporous Materials

journal homepage: www.elsevier.com/locate/micromeso

Development of antimicrobial hybrid mesoporous silver phosphate–pectin microspheres for control release of levofloxacin

Bernardo Bayón [a], Verónica Bucalá [b, c], Guillermo R. Castro [a, *]

[a] Nanobiomaterials Laboratory, Institute of Applied Biotechnology (CINDEFI, UNLP-CONICET, CCT La Plata), Dept. of Chemistry, School of Sciences, Universidad Nacional de La Plata, Calle 47y 115, 1900 La Plata, Argentina
[b] Planta Piloto de Ingeniería Química (PLAPIQUI), CONICET – Universidad Nacional del Sur (UNS), Camino La Carrindanga Km 7, 8000 Bahía Blanca, Argentina
[c] Departamento de Ingeniería Química, UNS, Avenida Alem 1253, 8000 Bahía Blanca, Argentina

A B S T R A C T

Pectin was used as nucleation agent in the synthesis of spherical mesoporous Ag_3PO_4 microspheres for the development of dual antimicrobial carrier containing a fluoroquinolone. The hybrid Ag_3PO_4–pectin microspheres were characterized by biophysical methods using optical, scanning and transmission electronic microscopies, X-ray diffraction and energy dispersive analysis, differential scanning calorimetry, laser diffraction, and molecular gas adsorption (Brunauer–Emmett–Teller). Scanning electron microscopy (SEM) images of silver phosphate microspheres without pectin displayed heterogeneous surface, bimodal size distribution between 0.9–1.0 μm and 1.5–1.8 μm with 20% and 25% population yield respectively and high amount of salt detritus. Meanwhile, SEM microphotographies of silver phosphate microspheres synthesized in presence of pectin showed a drastic change of particle morphology, homogenous surface, narrow size particle distribution in the 1.3–1.5 μm range with 90% population yield, 20–30% pore size increase and without debris. X-ray diffraction analysis of silver phosphate microspheres showed the same crystal profile in presence or absence of pectin suggesting no changes in the crystalline structure of Ag_3PO_4 by the addition of the biopolymer was made. Effect of silver phosphate hybrid microspheres loaded with levofloxacin tested against *Escherichia coli* and *Staphylococcus aureus* showed strong bactericidal activity compared with the bacteriostatic effect of free levofloxacin. The results are suggesting that hybrid Ag_3PO_4–pectin microspheres containing levofloxacin can be used as effective antimicrobial against several microorganisms, making them applicable to diverse medical devices and for antimicrobial control systems. The Ag_3PO_4–pectin hybrid microspheres are advantageous since they are synthesized by green chemistry methodology under standard laboratory conditions, do not requiring purification steps, the technique is highly reproducible and they are available for drug loading and specific target tailoring. The main advantage of Ag_3PO_4–pectin microspheres is the synergic antimicrobial activity of the silver ion and the antibiotic in the same microdevice acting as biocide matrix and also as carrier for levofloxacin.

© 2016 Elsevier Inc. All rights reserved.

1. Introduction

The emergency of multi-drug resistance (MDR) is a huge concern for human health at global scale [1]. For example, 450,000 new cases of MDR were reported in 92 countries only for tuberculosis in 2012. In particular, nosocomial microbial infections are serious obstacles everywhere for treatment of many microbial diseases [2]. Additionally, for many reasons the discovery, development and production of novel antibiotics were delayed over the last 30 years [3]. In order to solve the sanitary emergency, two main strategies for antimicrobials administration were established: the first one involves the development of novel and more effective drug carriers; and the second is the selection of two drug molecules with different microbiocide activity loaded together in the formulation [4].

Particularly, the interest of silver as antibacterial, used since ancient times, was recently rediscovered by the academy and extensively studied in last ten years [2,5]. The main advantages of

* Corresponding author. Tel./fax: +54 221 4833794x132/103.
E-mail address: grcastro@gmail.com (G.R. Castro).

silver devices are based on their low toxicity in humans, broad antimicrobial spectrum and low probability to produce bacterial resistance compared to traditional antibiotics. In fact, silver alone or combined with other molecules are currently used for controlling bacterial growth in a variety of applications, including dental implants, skin creams and patches, catheters, and clothes [6–8].

The strong silver biocide activity was attributed to several antimicrobial mechanisms such as damage of cell membrane proteins, blocking RNA transcription, disruption of DNA binding and replication [9]. Silver phosphate crystals with different morphologies synthesized in presence of detergent (Triton X-100) or polymers (polyacrylates or polyglycol 2000) were reported as bacteriostatic on *Escherichia coli* DH5α [10]. The antimicrobial mechanisms of silver phosphate crystals postulated by the authors were the membrane damage, ROS formation in the cytoplasm by the Ag^{1+} and interference on ATP synthesis by the silver salt [10]. Similarly, crushed code fish bones immersed into silver nitrate solution and dried showed high antimicrobial activity against *E. coli* and *Staphylococcus aureus* [11]. In another work, antimicrobial activity of hydroxyapatite containing silver was strongly correlated with the Ag^{1+} content. However, hydroxyapatite-silver particles higher than 45 nm or with high silver payload showed structural inhomogeneity and low antimicrobial activity against *S. aureus* and *Pseudomonas aeruginosa* [12]. Interestingly, no toxicity was found using calcium phosphate surfaces sprayed with silver nitrate on Chinese hamster V79 cell line [13]. Diverse silver phosphates morphologies and features such as amorphous to crystals structures showing from irregular spheroids to arrow-head morphologies in presence of ammonia (*i.e.* diamine−silver complex formation) were observed by SEM. In addition, polyhedral and cubic silver phosphate crystals were synthesized by modifying the reaction components and physicochemical parameters such as solvent polarity, the ratio of solvation (*e.g.* ethyleneglycol−water mixtures), temperature, etc [14–16]. Besides, SEM images of the reported silver phosphate salts showed medium to high polydispersity, and/or wide polymorphism and/or the presence of parasitic structures because of complicated intrinsic control of physicochemical experimental conditions. The particle polymorphism and high polydispersity are both serious drawbacks for the development of drug delivery carriers since it is not possible to establish a proper drug loading and controlled release profile.

In recent years, mesoporous silica-based materials, *e.g.* MCM-41 or SBA-15, loaded with wide range of antimicrobials from silver nanoparticles, antibiotics to lytic enzymes were explored for the development of microbiocide devices against fastidious and antibiotic resistant microorganisms [17,18]. The main advantages of mesoporous materials are the ability of absorb and contain many molecules with different molecular weights and physicochemical properties keeping their biological activities by tailoring pore diameter and/or chemical structure. The tuning of mesoporous structures is determining the interactions within the loads and consequently the controlled release kinetics [19].

Devices based on silver salts and polymers could improve antimicrobial activity against pathogens but only few reports were found in the literature and the mechanisms are not fully understood [20,21]. Biopolymers such as alginate, cellulose, pectin among others were lately reported as potential "green carriers" for drug delivery [22]. Natural polymers are providing excellent platforms for molecular loading and release because of gelling properties, and also considered smart molecules since they are sensitive to environmental conditions (*e.g.* pH, temperature, ionic strength). Most of biopolymers are non-toxic, degradable, showing high structural diversity and some of them are used in food or food supplements (*e.g.* fibers). Also, biopolymers displayed wide variety of functional groups easy to tailor by Green Chemistry techniques.

Particularly, pectins are water-soluble food-grade polysaccharides synthesized in plant cell walls. Pectins are linear poly-α-(1,4)-D-galacturonic acids chains partially methoxylated. Pectins are slowly degraded in humans by the intestinal flora, which can be considered advantageous for the development of intestinal drug delivery carriers [4]. In this sense, the use of biopolymers as nucleation agents for the development of hybrid inorganic matrices carrying biocides is a feasible alternative (*e.g.* encapsulation of ciprofloxacin in a matrix composed of $CaCO_3$ and carrageenans) [23]. Similar approach was reported for the synthesis of silver phosphate antimicrobial particles in presence of chitosan and hyaluronic acid, but the particles are displaying wide particle size distribution, and no biocide was incorporated into the device [24].

Fluoroquinolones are among the most used broad-spectrum antibiotics for Gram(+) and Gram(−) bacteria. The main mechanism of fluoroquinolones antimicrobial activity is based on the inhibition of topoisomerases (*e.g.* DNA gyrase and topoisomerase type IV) causing DNA breakage and consequently microbial cell death. Levofloxacin is a fluoroquinolone used to treat many bacterial infections (*e.g.* chronic bronchitis, sinusitis, conjunctivitis, and penicillin-resistant strains of *Streptococcus pneumonia*, etc.), urinary tract and abdominal infections, but also skin and soft tissue infections. However, some adverse effects of levofloxacin like gastrointestinal problems such as abdominal discomfort, anorexia and diarrhea were reported in clinical studies [25]. Additionally, fluoroquinolones are showing unwanted secondary side effects because of molecular stacking attributed to the aromatic ring structure and low solubility in aqueous media [26]. These main properties of fluoroquinolones are reducing the antibiotic biodisponibility and became toxic because of crystal formation inside the body [27].

The aim of the present work was to develop a simple and reproducible aqueous method for the synthesis of Ag_3PO_4 microspheres (AgP-Ms) in presence of pectin and loaded with levofloxacin as novel dual-antimicrobial device. The novel hybrid AgP-Ms were characterized by biophysical methods using optical, scanning and transmission electronic microscopies (OM, SEM and TEM), X-ray techniques like diffraction (XRD) and Energy Dispersive Analysis (EDAX), Differential Scanning Calorimetry (DSC), Laser Diffraction (LD), and molecular gas adsorption (Brunauer−Emmett−Teller, BET and Barrett−Joyner−Halenda, BHJ). Finally, the antimicrobial activity of AgP−pectin microspheres containing levofloxacin was tested against the Gram(+) *S. aureus* and the Gram(−) *E. coli* in agar plates, and also the microbial viability and minimal inhibitory concentrations (MIC) were determined in liquid medium.

2. Experimental

2.1. Materials

High Methoxylated Pectin (HMP, ED 74%, average $M\eta$ 1.60×10^5 Da) was kindly provided by C.P. Kelco (Buenos Aires, Argentina). All other reagents used were of analytical grade purchased from Sigma (St. Louis, MO) or Merck (Darmstadt, Germany) or from local suppliers. Deionized water was prepared using reverse osmosis equipment Aqual 25 (Brno, Czech Republic) and further purified by using a MiliQ Direct QUV apparatus equipped with a UV lamp.

2.2. Silver phosphate microspheres synthesis

Silver phosphate microspheres (AgP-Ms) containing or not high methoxylated pectin (HMP) were made by precipitation. Briefly, 9.0 ml of 100 mM $AgNO_3$ solution was quickly added to 9.0 ml of

60 mM sodium tripolyphosphate ($Na_5P_3O_{10}$) with or without 2.0 ml of 1.0% HMP at room temperature under stirring for 5 min. The precipitate was centrifuged (4000 × g, 10 min) and washed twice with one volume of MiliQ water. The supernatant were discarded and the microspheres obtained were lyophilized (Rificor L3, Argentina) and kept under the dark.

2.3. X-ray diffraction (XRD)

Dried sample diffraction patterns were collected using Analytical Expert Instrument (Philips 3020, The Netherlands) using CuK_α radiation ($\lambda = 1.54$ Å) and scans in the 2θ range $20° \le 2\theta \le 90°$ with 0.04 step size and 1.00 seg/step at room temperature. The generator tension was 40 kV and current of 35 mA. The sizes of AgP-Ms were determined by the Scherrer equation:

$$L = \frac{K \cdot \lambda}{\beta \cdot \cos \theta}$$

where $K = 1$, assuming spherical particles; β is the width at half maximum intensity of the reflection, θ is Bragg's angle and $\lambda = 1.54$ Å is the wavelength of the X-ray radiation.

2.4. Differential scanning calorimetry (DSC)

The calorimetrical analyses were made using a TA-Instrument calorimeter (model Q2000 V24.10 Build 122; New Castle, DE, USA). The temperature was scanned at heating rate of 10 °C/min from 20 °C to 250 °C range under nitrogen atmosphere. Each experiment was performed by triplicate.

2.5. Morphology and structural analysis of the particles by optical microscopy

The AgP-Ms were analyzed using an optical microscope at 10×, 40× and 100× magnifications (Leica DM 2500, Germany), under different experimental conditions: humid, lyophilized and rehydrated.

2.6. Morphology and structural particle analysis by scanning electron microscopy (SEM)

SEM analysis was performed using freeze-dried AgP-Ms for 72 h and stored in desiccators under dark conditions. The samples were prepared by sputtering the surface AgP-Ms with gold using a Balzers SCD 030 metalizer with layer thickness between 15 and 20 nm. Particles surfaces and morphologies were observed using Philips SEM 505 model (Rochester, USA), and processed by an image digitalizer program (Soft Imaging System ADDA II (SIS)).

The size distribution, diameter and surface roughness of the AgP-Ms SEM images were analyzed by ImageJ software (NIH, USA). The roughness of the surface was estimated by the standard variation of the gray values of all the pixels on the image. The less the standard variation value is, the smoother the surface is [31]. The histograms were performed by duplicate of SEM images at 5000× magnification.

2.7. Energy dispersive X-ray analysis (EDAX)

Chemical analysis by EDAX analysis was performed using Apex 2 EDAX Apollo X coupled to SEM in dried samples.

2.8. Nitrogen adsorption isotherms (BET and BHJ analysis)

Nitrogen adsorption−desorption were carried out in dry microspheres at 77 K. Surface area, pore volume and pore size of the different formulations were estimated using the Micromeritics ASAP 2020V3.00 Software by applying the Brunauer−Emmett−-Teller (BET) equation and the Barrett−Joyner−Halenda (BJH) technique.

2.9. Transmission electron microscopy (TEM) analysis

The AgP-Ms were analyzed by TEM to determine morphology and size. A volume of suspended AgP-Ms (1.0 mg/ml) at room temperature was removed and applied to a collodion-coated Cu grid (400-mesh). Liquid excess was drained with filter paper. Images were obtained in a Jeol-1200 EX II-TEM microscope (Jeol, MA, USA).

2.10. Laser diffraction (LA)

Particle size distribution was measured using a laser light diffraction instrument (LA 950 V2, Horiba). Particle size distributions are reported as normalized mass histograms and cumulative distributions. Also representative sizes d_{10}, d_{50} (median mass size) and d_{90} were calculated from the normalized cumulative mass passing distributions. d_{10}, d_{50} and d_{90} represent the opening sizes that would let pass 10, 50 and 90 wt% of the sample, respectively. The distribution width was characterized in terms of span. The span index was calculated as follows:

$$\text{Span} = \frac{(d_{90} - d_{10})}{d_{50}} \tag{1}$$

Span values lower than 2 indicate relatively narrow particle size distributions [29].

2.11. Antibacterial studies

2.11.1. Microbial cultures
S. aureus (ATCC 6538) and *E. coli* (ATCC 25922) were cultured in nutrient broth medium at 100 rpm and 37 °C for 12 h.

2.11.2. Assays of AgP-Ms antimicrobial activity in agar plates
Inhibition zones against *S. aureus* and *E. coli* were determined by using modified disk diffusion method in agar plates according to CLSI/NCCLS, replacing the disks for sterile glass cylinders. The glass cylinders were further placed on the inoculated agar plate surface. Solutions containing 1.0 µg/ml of AgP-Ms and further dilutions were tested. Each solution (25 µl) was placed inside the cylinders on the plates and incubated at 37 °C and then the inhibition zones were determined after 24 h.

2.11.3. Levofloxacin loading
The microspheres were charged with Levofloxacin (Levo) by placing 10.0 mg of lyophilized microspheres into a 1.0 mg/ml solution of the drug at room temperature under slow agitation for 24 h. After loading, the microspheres were centrifuged at 10,000 × g for 5 min and them the precipitates were washed with miliQ water two times. The particles were resuspended in water miliQ, this solution was then used for the antimicrobial essays.

2.11.4. Antimicrobial assays using AgP-Ms loaded with levofloxacin (levo)
Antimicrobial activity against *E. coli* and *S. aureus* was performed as mentioned before (see Section 2.11.2). Solutions

containing 1.0 mg/ml of AgP-Ms with and without pectin, AgP-Ms with and without pectin loaded with Levo and free drug control were analyzed.

2.11.5. Viability essays in nutrient broth

E. coli and *S. aureus* were cultivated in 50 ml Erlenmeyer flasks containing nutrient broth at 37 °C and used to compare the antimicrobial activity between the free drug and the drug-loaded microspheres. Bacterial cultures were followed up to the half exponential phase, and them particles loaded with Levo or free drug were added to the flasks. Upon completion of 24 h culture aliquots of 100 μl were taken and spread on Petri dishes containing Mueller Hinton agar incubated at 37 °C. The bacterial survival was estimated by UFC/ml count on the agar plates. Controls of bacterial growth in absence of Levo, with increasing free antibiotic concentrations (from 5.0 to 10.0 μg/ml) and with unloaded antibiotic microspheres were carried out. The bacterial inhibition growth was also measured by optical density at 600 nm.

2.12. Statistical analysis

All experiments were carried out at least in triplicates. The mean values were analyzed by the one way analysis of variance (ANOVA) with a significance level of 5.0% ($p < 0.05$) followed by Fisher's least significant difference test ($p < 0.05$).

3. Results and discussion

3.1. Synthesis of Ag_3PO_4 hybrid microspheres

Colloidal precipitation of AgP-Ms with or without 0.1% (w/v) HMP under our experimental conditions resulted in microspheres determined by optical microscopy (Fig. 1). However, SEM and TEM micrographs showed lyophilized fine microspheres powders with different morphologies and surfaces depending on the presence or absence of pectin. SEM micrographs confirmed spherical shapes of AgP-Ms but also are providing significant evidence of the relevant role of pectin during AgP-Ms synthesis (Fig. 2). In absence of pectin, the Ag-Ms microspheres synthesis is producing many salt detritus, particle aggregation and irregular surface (Fig. 2A). On the other side, images of AgP-Ms synthesized in presence of pectin revealed spherical shape, more uniform and narrow size dispersion with increased smooth surface (Fig. 2B). Besides the spherical shape was conserved, new distinctive surface pattern appeared when pectin is present during microparticle synthesis. This characteristic was also observed in the TEM images (Fig. 3): smooth surface architecture

was evidenced in the AgP—pectin microspheres indicating a crucial role of biopolymer during the silver salt nucleation and particle formation. In this sense, AgP—Pectin microspheres could expose pores in the surface occupied by pectin chains, creating an interesting pattern made by the polymer coat. Energy-dispersive X-ray spectroscopy (EDAX) analysis of the silver phosphate microspheres containing or not pectin displayed the same profile distribution suggesting that chemical composition for both types silver phosphate salt was unaltered by the presence of the biopolymer during the microparticle synthesis (Fig. 1S, Supplementary material).

3.2. Size distribution of SPP's beads

SEM micrographs and ImageJ software analysis showed an average diameter of dried AgP-Ms containing HMP in the range of 1.30—1.50 μm with population yield higher than 90% and without noticeable salt detritus (Fig. 2B). On the contrary, dried AgP-Ms synthesized in absence of pectin showed a wide and bimodal particle size distribution (Fig. 2A). The top particle distributions of AgP-Ms without pectin were in the range of 0.9—1.0 μm and 1.5—1.8 μm diameter but also with very low population yields of about 20% and 25% respectively (Fig. 4). Surface analysis of the AgP—pectin microspheres by ImageJ program showed about 30% lower standard deviation compared to the same microspheres without the biopolymer which are indicating smooth surface for the AgP—pectin microspheres (Fig. 2S, Supplementary material). Similar trends were observed in the $CaCO_3$ microspheres synthesized in presence or absence of λ-carrageenans [27].

3.3. Laser diffraction (LD)

The median size of microspheres determined using LD doesn't match the particle size observed in the SEM images. The reason of the discrepancy is because of LD analyze ionic radius which is usually bigger than real particle size. Silver phosphate microspheres showed asymmetric size distribution tailed to large diameters (Fig. 5A). In contrast AgP—pectin microspheres showed Gaussian type distribution (Fig. 5B). Silver phosphate microspheres showed asymmetric size distribution tailed to large diameters with maximum medium size (d_{50}) of 1.57 μm. In contrast AgP—pectin microspheres showed Gaussian type distribution with maximum medium size (d_{50}) of 2.41 μm. The increase of medium size of the AgP—pectin microspheres could be attributed to the presence of the polymer in microspheres and the contribution of residual electric charges of the biopolymer in the microsphere surface. The biopolymer lead to a narrower distribution, in fact the distribution
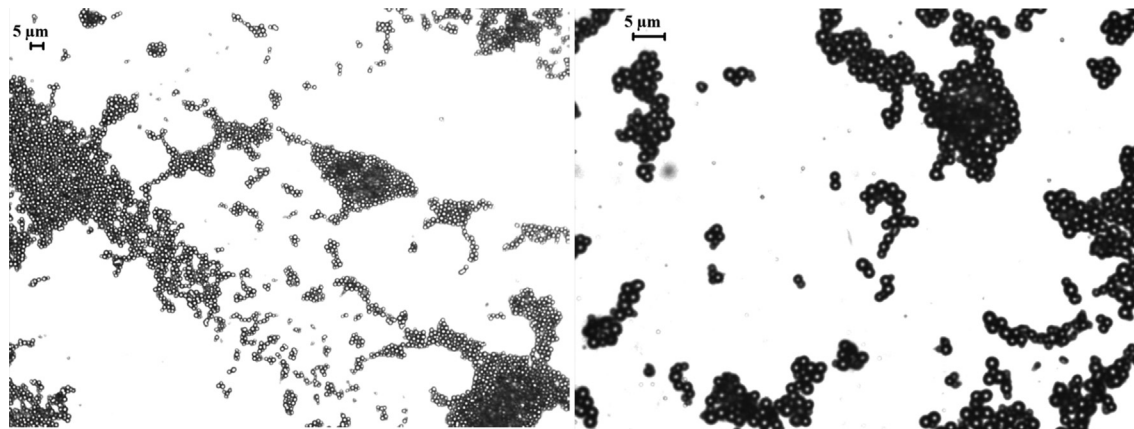

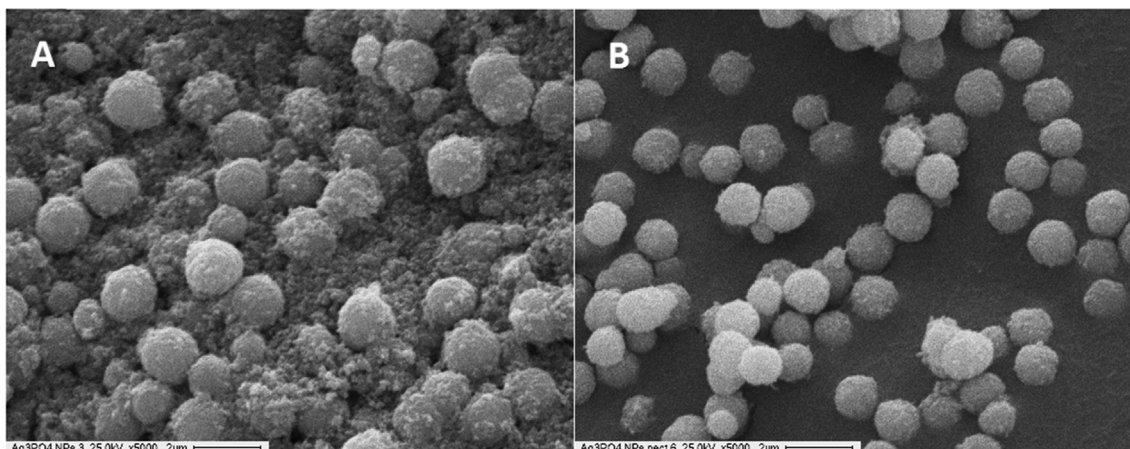**Fig. 1.** Optical microscopy of the silver phosphate—pectin microspheres: (a) 40×; (b) 100×.

Fig. 2. SEM images of silver phosphate microspheres in absence (A) and in presence of pectin (B) at 5000× magnification.
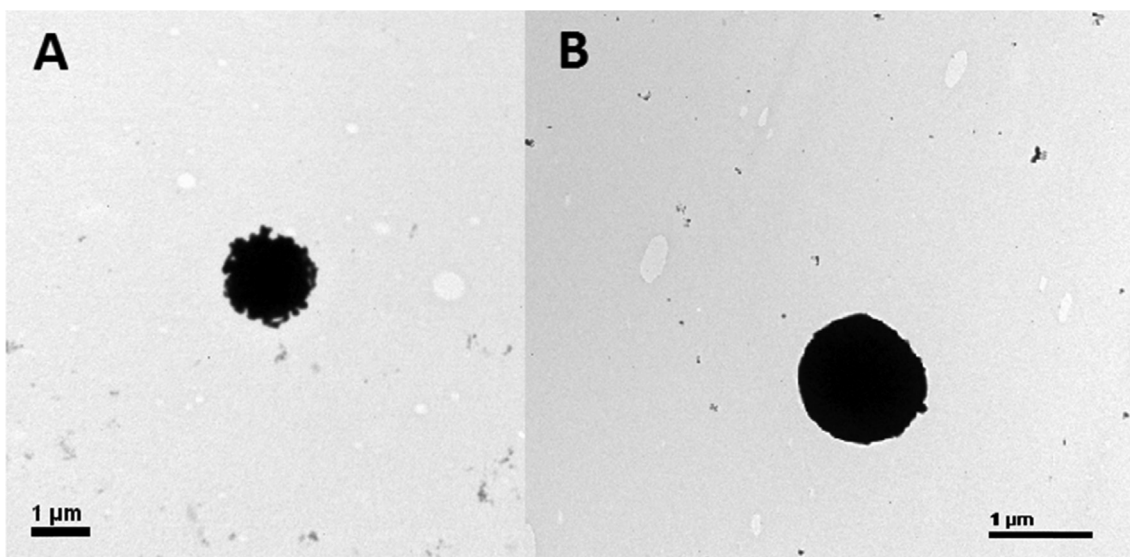

Fig. 3. TEM images of silver phosphate microspheres synthesized in absence (A) and in presence of pectin (B) at different magnifications 10,000× (A) and 20,000× (B).
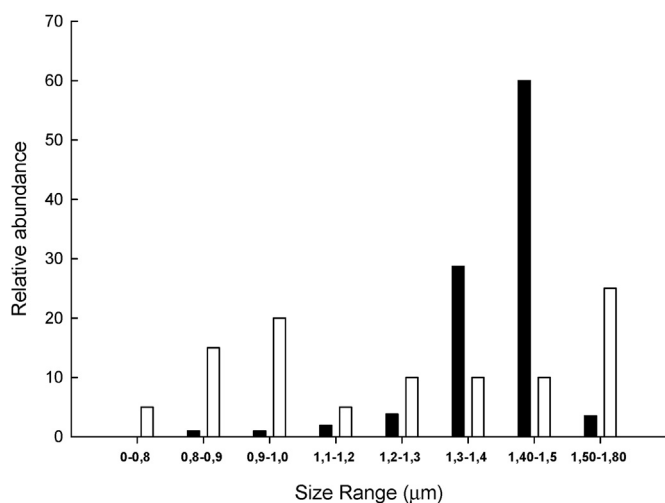

Fig. 4. Shape and size distribution of Ag_3PO_4 microspheres with (■) and without (□) pectin.

span for AgP–Pectin-Mps was 1.4 while for samples without pectin was about 2.0 (Table 3S).

3.4. Structural analysis of the particles using XRD

The AgP-Ms structure was evaluated by X-ray diffraction analysis of the microspheres containing or not Pectin (Fig. 6). The presence of the peak at 33° with highest intensity was assigned to (210) plane in the XRD of Ag_3PO_4 microspheres and it is the characteristic peak of silver phosphate [31]. Also, the diffractograms showing the same spectrum profile for both type of samples which are strongly suggests that the crystal structure of the AgP-Ms containing pectin was unchanged.

3.5. Nitrogen adsorption isotherms (BET)

Determination of the microspheres porosity was carried out by N_2 adsorption and desorption at 77 K (Table 1). Gas adsorption in the P/Po range of 0.1–0.3 gave a specific surface area of 74 $m^2 g^{-1}$ of Ag_3PO_4 particles, meanwhile 43 $m^2 g^{-1}$ for AgP–Pectin microspheres. The high surface area suggested the presence of nanopores
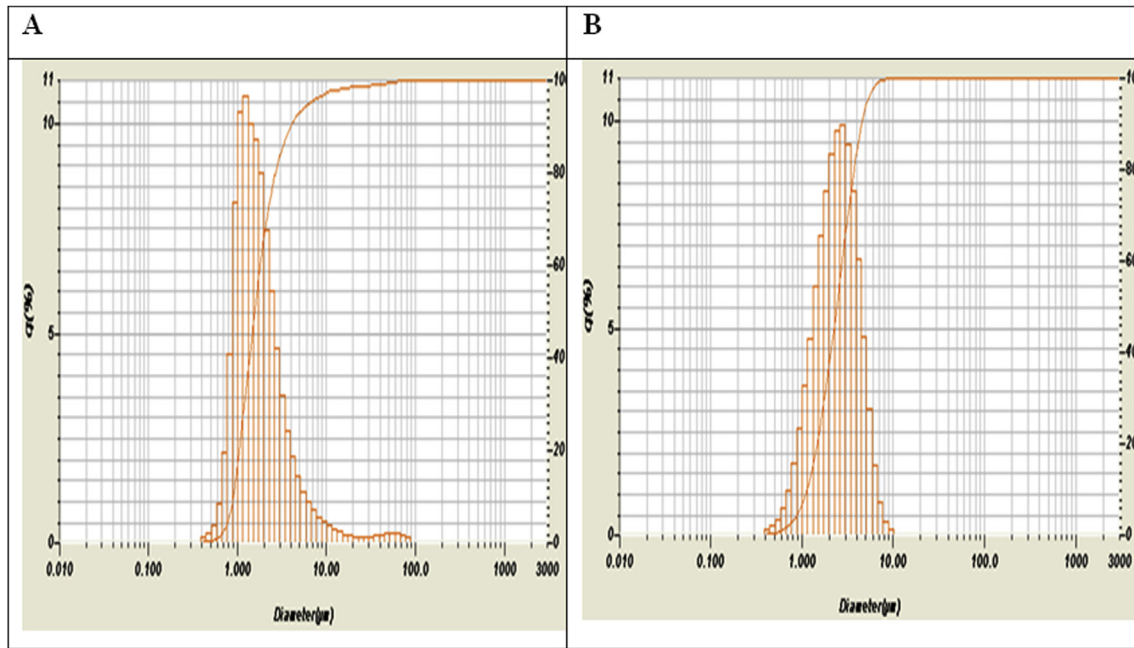
Fig. 5. Normalized mass size distributions of silver phosphate microparticles without (A) or with (B) pectin determined by laser diffraction.
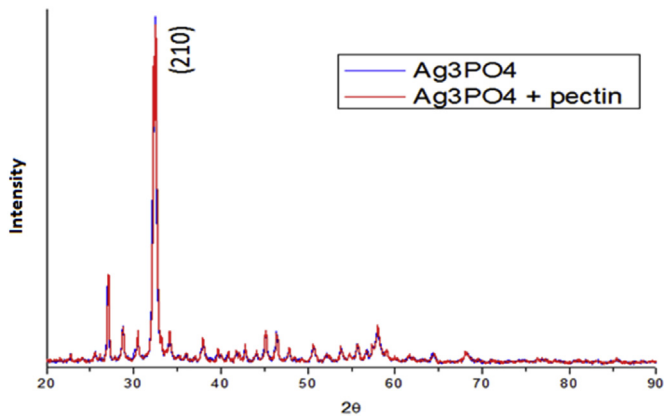

Fig. 6. Particle X-ray diffraction analysis.

within the particle structure. This could be also observed in the hysteresis obtain of the isotherm linear plot graph, characteristic place in the mesoporous materials. Analysis of the matrices showed between 19% and 34% pore size increase by the addition of pectin to the mesoporous microparticle synthesis (Table 1). The smaller surface area and pore volume for AgP–Pectin microspheres can be attributed to the pectin, which would led to less but wider pores than the observed for AgP-Ms. Also, this hypothesis is in agreement with the smooth surface determined in the microspheres by ImageJ analysis of SEM microphotographies. These results are suggesting

that the polymer is covering the particle surface making it smoother and making wider pores.

3.6. Thermal properties using DSC

The thermal analysis with DSC studies was performed in order to confirm the hypothesis of Ag_3PO_4/pectin interactions and the presence of pectin in the microspheres. The thermogram of AgP–pectin microspheres showed an exothermic peak at approximately 110 °C corresponding to the melting point of pectin incorporated in particles nanostructure. However, no peaks were observed in the silver phosphate microspheres thermogram profile. Also, pectin showed the characteristic profile with the smooth endothermic peak (Fig. 4S, Supplementary material).

3.7. Antibacterial study against Gram positive and Gram negative strains

3.7.1. Zone of inhibition

Antimicrobial activity of the AgP microspheres were tested on agar plates containing the typical Gram(+) and Gram(−) microorganisms *S. aureus* and *E. coli* respectively.

Comparison of 0.50 mg/ml AgP-Ms antimicrobial activity with and without pectin in agar plates showed similar results for both bacterial strains tested (Fig. 5S). The antimicrobial capability of AgP-Ms containing pectin tested against *S. aureus* and *E. coli* are confirming the antimicrobial activity of silver in particles.

Table 1
Characterization of microspheres by nitrogen adsorption isotherms (BET). In all cases standard deviation is lower than 5.0%. BJH adsorption cumulative volume of pores between 1.7 nm and 300.0 nm width.

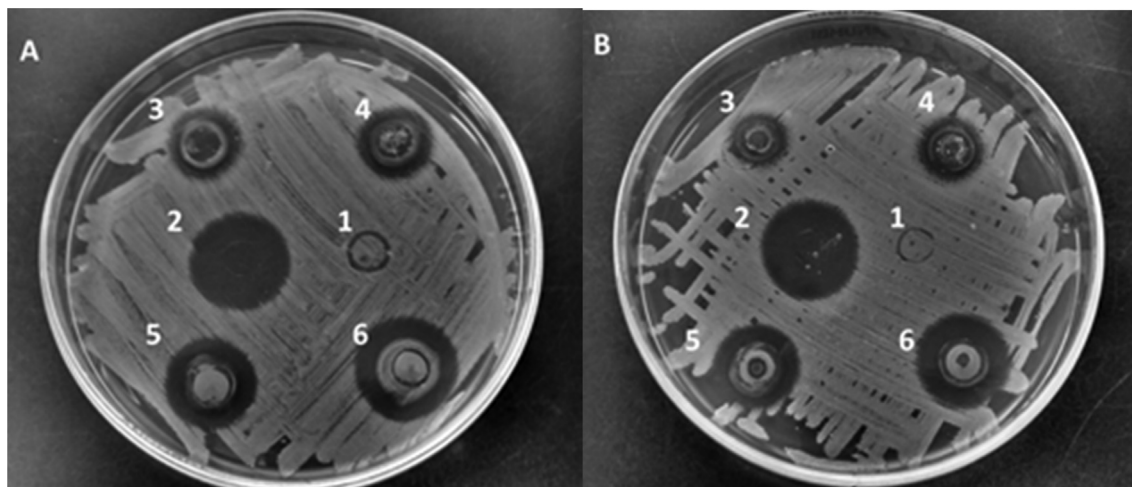| Microsphere sample	Surface area (m²/g)	Pore volume (cm³/g)	Pore size (nm)	
			BJH adsorption	BET method
AgP	74.04	0.24	12.34	13.07
AgP–Pectin	43.21	0.17	16.57	15.56

Fig. 7. Antimicrobial assay in agar plates using dilutions of the Ag₃PO₄ microspheres (AgP-Ms). Microorganisms: (a) *Escherichia coli* (b) *Staphylococcus aureus*. (Particles Stock: 5.0 mg/ml; wells: (1) control with water; (2) control Levo (1.0 mg/ml); (3) AgP-Ms; (4) AgP–pectin Ms; (5) AgP-Ms loaded with Levo; (6) AgP–pectin Ms loaded with Levo.

3.7.2. Antimicrobial assay using AgP-Ms loaded with levofloxacin (levo)

Furthermore, Levofloxacin was loaded into the silver microspheres to test antimicrobial activity. The biocide activity of AgP-Ms containing or not pectin was enhanced by the presence of levofloxacin (Fig. 7). Comparative microbial inhibition diameter between free and encapsulated levofloxacin do not show differences, suggesting no interference by the presence of the formulation components of the microspheres, silver ion and pectin in the biocide activity.

Additionally, the loading capability of silver microspheres containing pectin was enhanced and attributed to the interaction between the fluoroquinolone and biopolymer similarly as previously reported in the case of ciprofloxacin and alginate [24,30].

3.7.3. Viability test in nutrient broth

Samples of batch cultures of *E. coli* and *S. aureus* cultivated one day in presence or absence of levo and silver microspheres loaded with levo were spread in agar plates and incubated at 37 °C for 12 h. The plates are indicating some microbial growth after incubation with levofloxacin during 24 h, meanwhile no viable cells were found in the cultures exposed to silver phosphate microspheres loaded with the fluoroquinolone (Fig. 8 and Table 2).

4. Conclusions

Spherical hybrid mesoporous Ag₃PO₄–pectin microspheres were successfully synthesized using reproducible and facile precipitation method under physicochemical controlled conditions.
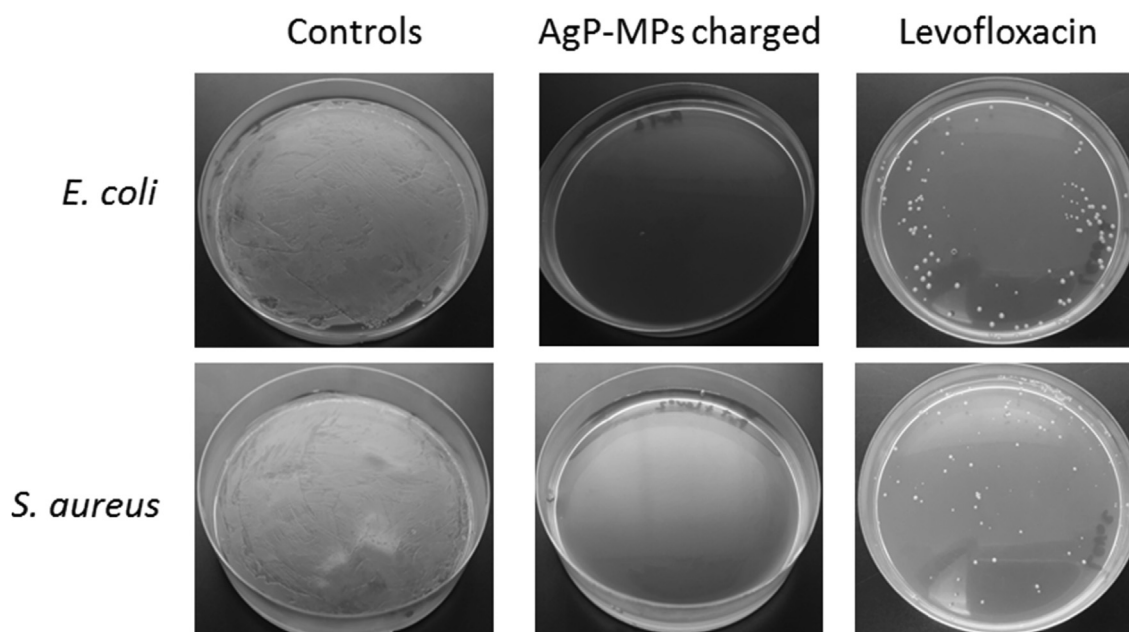

Fig. 8. Viability counting assay in agar plates using Ag₃PO₄–pectin microspheres loaded with levofloxacin and free drug, against *Escherichia coli* and *Staphylococcus aureus*. (Particles: 1.0 mg/ml; Levo: 10.0 μg/ml, controls in absence of any antimicrobial agent).

Table 2
Colony counting of the viability assays corresponding to the pictures of Fig. 8.

Microorganism	Bacterial control	AgP–pectin Ms (UFC/ml)	Levofloxacin (UFC/ml)
E. coli	Lawn	0	920 ± 60
S. aureus	Lawn	0	825 ± 40

The antimicrobial activity is directly related to structure of the mesoporous microspheres which is advantageous since its high intrinsic crystal stability compared to the silver loaded silica mesoporous structures.

The formation of mesoporous silver phosphate–pectin hybrid microspheres are displaying well-defined spherical shape and narrow size distribution confirmed by diverse microscopy techniques (OM, SEM and TEM) and LD. X-ray diffraction of AgP–pectin microspheres showed no changes in the crystal structure of Ag_3PO_4 in the presence of pectin. However, the inclusion of pectin into AgP-Ms produces a reduction almost in half in microparticle surface and almost in one third in pore diameter, but increase in about 25% the pore size determined by BJH and BET techniques. Another advantage of the AgP–pectin microspheres is the absence of salt detritus and the enhanced incorporation of levofloxacin into the microspheres. Additionally, the amount of the loaded antibiotic can be tuned based on the pectin content in the mesoporous microspheres which is advantageous since can make a versatile drug delivery device for different therapeutic purposes.

The AgP–pectin microspheres loaded with levofloxacin showed an increased biocide activity against *E. coli* and *S. aureus*. The results demonstrate that microbial cultures exposed to 1.0 mg/ml levofloxacin contains viable microbial cells after 24 h incubation, meanwhile no viable cells were detected in presence of silver phosphate hybrid microspheres loaded with the antibiotic. The main advantage of AgP–pectin microspheres is the synergic antimicrobial effect of silver ion with the antibiotic in the same microdevice with dual function: acting as biocide matrix and as carrier for levofloxacin. The enhanced antimicrobial activity of AgP–pectin device containing levofloxacin allowed to diminish the antibiotic concentration in the dose and consequently decreasing the potential undesirable antibiotic side effects favoring patient compliance.

Mesoporous silver phosphate microspheres containing pectin can be synthesized by Green Chemistry technical approach in a simple, reproducible and cost-effective manner and they are suitable for formulation of new types of dual bactericidal materials containing also others molecules. Application of antibacterial silver phosphate–pectin microspheres may be useful on the treatment of skin infections or in diverse industrial fields such as textiles, coatings, paintings, and medical devices.

Acknowledgments

Appendix A. Supplementary material

Supplementary data related to this article can be found at http://dx.doi.org/10.1016/j.micromeso.2015.12.041.

References

[1] C. Llor, L. Bjerrum, Ther. Adv. Drug Saf. 5 (2014) 229–241, http://dx.doi.org/10.1177/2042098614554919.

[2] O. Choi, K.K. Deng, N.-J. Kim, L. Ross, R.Y. Surampalli, Z. Hu, Water Res. 42 (2008) 3066–3074, http://dx.doi.org/10.1016/j.watres.2008.02.021.

[3] WHO, Antimicrobial Resistance: Global Report on Surveillance, 2014 (n.d.), http://www.who.int/drugresistance/documents/surveillancereport/en/ (accessed 13.04.15).

[4] L. Costas, L.M. Pera, A.G. López, M. Mechetti, G.R. Castro, Appl. Biochem. Biotechnol. 167 (2012) 1396–1407, http://dx.doi.org/10.1007/s12010-012-9615-x.

[5] W.-R. Li, X.-B. Xie, Q.-S. Shi, H.-Y. Zeng, Y.-S. Ou-Yang, Y.-B. Chen, Appl. Microbiol. Biotechnol. 85 (2010) 1115–1122, http://dx.doi.org/10.1007/s00253-009-2159-5.

[6] C.Y. Flores, C. Diaz, A. Rubert, G.A. Benítez, M.S. Moreno, M.A. Fernández Lorenzo de Mele, et al., Spontaneous adsorption of silver nanoparticles on Ti/TiO₂ surfaces. Antibacterial effect on *Pseudomonas aeruginosa*, J. Colloid Interf. Sci. 350 (2010) 402–408, http://dx.doi.org/10.1016/j.jcis.2010.06.052.

[7] Q. Li, X. Li, Nanosilver Particles in Medical Applications: Synthesis, Performance, and Toxicity, 2014, pp. 2399–2407.

[8] X. Chen, H.J. Schluesener, Toxicol. Lett. 176 (2008) 1–12, http://dx.doi.org/10.1016/j.toxlet.2007.10.004.

[9] P.D. Marcato, R. De Conti, O.L. Alves, F.T.M. Costa, M. Brocchi, Potential Use of Silver Nanoparticles on Pathogenic Bacteria, Their Toxicity and Possible Mechanisms of Action, vol. 21, 2010, pp. 949–959.

[10] J.-K. Liu, C.-X. Luo, J.-D. Wang, X.-H. Yang, X.-H. Zhong, Cryst. Eng. Commun. 14 (2012) 8714–8721, http://dx.doi.org/10.1039/c2ce25604e.

[11] C. Piccirillo, R.C. Pullar, D.M. Tobaldi, P.M. Lima Castro, M.M. Estevez Pintado, Ceram. Int. 41 (2015) 10152–10159, http://dx.doi.org/10.1016/j.ceramint.2015.04.116.

[12] J. Buckley, A.F. Lee, L. Olivi, K. Wilson, J. Mater. Chem. 20 (2010) 8056–8063, http://dx.doi.org/10.1039/c0jm01500h.

[13] Y. Ando, H. Miyamoto, I. Noda, N. Sakurai, T. Akiyama, Y. Yonekura, et al., Mater. Sci. Eng. C 30 (2010) 175–180, http://dx.doi.org/10.1016/j.msec.2009.09.015.

[14] Y. Bi, H. Hu, S. Ouyang, G. Lu, J. Cao, J. Ye, Chem. Commun. 48 (2012) 3748, http://dx.doi.org/10.1039/c2cc30363a.

[15] X. Guo, C. Chen, S. Yin, L. Huang, W. Qin, J. Alloys Compd. 619 (2015) 293–297, http://dx.doi.org/10.1016/j.jallcom.2014.09.065.

[16] B. Wang, L. Wang, Z. Hao, Y. Luo, Catal. Commun. 58 (2015) 117–121, http://dx.doi.org/10.1016/j.catcom.2014.09.013.

[17] L. Wang, H. He, C. Zhang, L. Sun, S. Liu, R. Yue, J. Appl. Microbiol. 116 (2014) 1106–1118, http://dx.doi.org/10.1111/jam.12443.

[18] D. Steri, M. Monduzzi, A. Salis, Micropor. Mesopor. Mater. 170 (2013) 164–172, http://dx.doi.org/10.1016/j.micromeso.2012.12.002.

[19] S.-Y. Park, M. Barton, P. Pendleton, Colloids Surf. A Physicochem. Eng. Asp. 385 (2011) 256–261, http://dx.doi.org/10.1016/j.colsurfa.2011.06.021.

[20] R. Ladj, A. Bitar, M.M. Eissa, H. Fessi, Y. Mugnier, R. Le Dantec, et al., Int. J. Pharm. 458 (2013) 230–241, http://dx.doi.org/10.1016/j.ijpharm.2013.09.001.

[21] Y. Murali Mohan, K. Vimala, V. Thomas, K. Varaprasad, B. Sreedhar, S.K. Bajpai, et al., J. Colloid Interf. Sci. 342 (2010) 73–82, http://dx.doi.org/10.1016/j.jcis.2009.10.008.

[22] C. Alvarez-Lorenzo, B. Blanco-Fernandez, A.M. Puga, A. Concheiro, Adv. Drug Deliv. Rev. 65 (2013) 1148–1171, http://dx.doi.org/10.1016/j.addr.2013.04.016.

[23] G.A. Islan, M.L. Cacicedo, V.E. Bosio, G.R. Castro, J. Colloid Interf. Sci. 439 (2015) 76–87, http://dx.doi.org/10.1016/j.jcis.2014.10.007.

[24] D. Chudobova, L. Nejdl, J. Gumulec, O. Krystofova, M.A.M. Rodrigo, J. Kynicky, et al., Int. J. Mol. Sci. 14 (2013) 13592–13614, http://dx.doi.org/10.3390/ijms140713592.

[25] R. Davis, H.M. Bryson, Levofloxacin. A review of its antibacterial activity, pharmacokinetics and therapeutic efficacy, Drugs 47 (1994) 677–700. http://www.ncbi.nlm.nih.gov/pubmed/7516863 (accessed 27.08.15).

[26] J.H. Paton, D.S. Reeves, Fluoroquinolone antibiotics. Microbiology, pharmacokinetics and clinical use, Drugs 36 (1988) 193–228. http://www.ncbi.nlm.nih.gov/pubmed/3053126 (accessed 27.08.15).

[27] G.A. Islan, I.P. De Verti, S.G. Marchetti, G.R. Castro, Appl. Biochem. Biotechnol. 167 (2012) 1408–1420, http://dx.doi.org/10.1007/s12010-012-9610-2.

[29] F. Palazzo, S. Giovagnoli, A. Schoubben, P. Blasi, C. Rossi, M. Ricci, Int. J. Pharm. 440 (2013) 273–282, http://dx.doi.org/10.1016/j.ijpharm.2012.05.045.

[30] V.E. Bosio, M. Cacicedo, B. Calvignac, I. Leon, T. Beuvier, F. Boury, G.R. Castro, Colloids Surf. B Biointerf. 123 (2014) 158–169, http://dx.doi.org/10.1016/j.colsurfb.2014.09.011.

[31] M. Kim, Y. Suh, J. Jeong, J. Lee, Hydrometallurgy 98 (2009) 45–51, http://dx.doi.org/10.1016/j.hydromet.2009.03.013.